

Contents lists available at [ScienceDirect](#)

Urban Forestry & Urban Greening

journal homepage: www.elsevier.com/locate/ufug

Thermal benefits of vertical greening in a high-density city: Case study of Hong Kong

Tobi Eniolu Morakinyo^{a,*}, Alan Lai^b, Kevin Ka-Lun Lau^a, Edward Ng^{a,b}

^a Institute of Future Cities, The Chinese University of Hong Kong, New Territories, Hong Kong

^b School of Architecture, The Chinese University of Hong Kong, New Territories, Hong Kong

ARTICLE INFO

Keywords:

ENVI-met

High-density

Thermal comfort

Temperature reduction

Vertical greening

ABSTRACT

To improve outdoor thermal environment and reduce indoor energy use, passive techniques including façade greenery have been suggested. In high-density cities like Hong Kong, buildings' surface area is much greater than the roof and ground surface areas combined, offering a huge vertical surface platform for greening. However, scientific evidence to assert the thermal benefit from this greening option especially at neighborhood scale is still very few. Therefore, this study was designed to provide such evidence using results from validated ENVI-met model simulation. Thereafter, parametric study was conducted to investigate the quantity and location of facade greening required for potential air cooling and thermal comfort improvement of a neighborhood of varying densities. Model validation results revealed an acceptable modelling of facade surface temperature, air temperature, relative humidity and wall-emitted long-wave fluxes. From the parametric study, we found that 30–50% of facades in the high-density urban setting of Hong Kong must be greened to potentially cause ~1 °C reduction in both daytime and nighttime air temperature while the same could help improve daytime pedestrian thermal comfort by at least one thermal class. We also established that higher greened facade ratio will be required to obtain similar thermal benefits in low and medium density urban settings. Also, realized benefits at pedestrians' height can be enhanced when the vertical greening facilities are placed along podium than tower heights. Lastly, practicable urban planning recommendations were presented for the attention of urban planners and landscape architects.

1. Introduction

Population growth in urban areas is projected to increase from 54% to 66% between 2014 and 2050 (UNF for Population Activities, 2010). To accommodate this, new buildings are rising resulting in an increase of impervious surfaces at the detriment of vegetated landscapes (Lo et al., 1997) and causing alterations to the processes of water, mass, and energy exchanges between the land surface and overlying air. Thus, urban microclimate is being modified, giving rise to the Urban Heat Island effect (UHI), which is associated with an increase in intra-urban temperatures and thermal stress when compared to surrounding rural areas (Oke, 1973; Brysse et al., 2013). Consequentially, heat stress condition has been prevalent and aggravating in summer months of cities, leading to increased rate of heat-related mortality (Lin et al., 2010, 2012; Tan et al., 2013). Among other techniques to mitigate this thermal discomfort is the introduction of urban vegetation i.e. ground level trees, green roof and vertical landscapes i.e. façade greening or green walls. Based on the fact that building surface area (especially in high-density cities like Hong Kong) is much greater than the roof and

ground surface area combined, greened building facades could offer enormous thermal benefits as understood from the underlying physical mechanism (Wilmers, 1990; Tan et al., 2014): reduced solar heat gain by leaves, followed by conversion of absorbed solar heat to latent heat by evapotranspiration, and finally, the reduction of absorbed radiation results in a lower surface temperature and thus less emitted longwave radiation. Therefore, the application of vegetated surfaces on the building facades i.e., vertical greening, could be harnessed in improving the microclimate around buildings and human thermal comfort in the built environment, particularly in the high density cities as Hong Kong with limited ground area for tree-planting.

The cooling effects of vertical or facade greening, on ambient indoor/outdoor air temperature and surface temperature have been widely investigated by both modelling and measurements methods (Tan et al., 2014; Holm, 1989; Takakura, 2000; Stec et al., 2005; Alexandri and Jones, 2008; Eumorfopoulou and Kontoleon, 2009; Kontoleon and Eumorfopoulou, 2010; Susorova et al., 2013; Cuce, 2017; De Jesus et al., 2017; Yin et al., 2017; Wong et al., 2009, 2010). The results are not always comparable due to different prevalent

* Corresponding author.

E-mail address: tobimorak@cuhk.edu.hk (T.E. Morakinyo).

<https://doi.org/10.1016/j.ufug.2017.11.010>

Received 12 September 2017; Received in revised form 15 November 2017; Accepted 16 November 2017

1618-8667/ © 2017 Elsevier GmbH. All rights reserved.

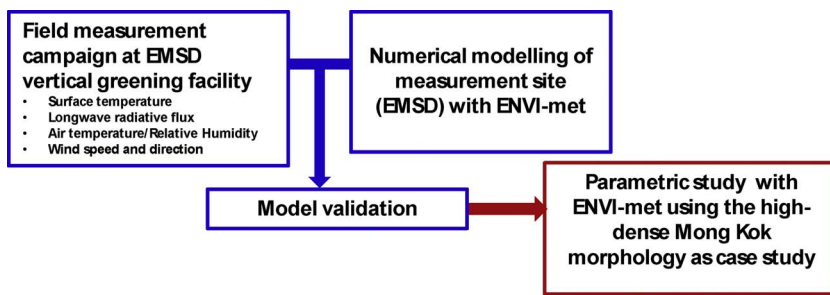


Fig. 1. Methodological framework of the study.

climate, applied methodology and walls material and orientation in the studies. Through simulation, [Holm \(1989\)](#) found a west-facing façade greening in hot-arid summer climate effective as maximum indoor air temperature reduced by 1 °C–4 °C. [Alexandri and Jones \(2008\)](#) simulated the effect of green wall and green roof on in-canyon air temperature under different climates. Their results shows disparity in air temperature reductions by green infrastructures in different climate. For instance, in hot-dry climate of Riyadh, daytime air temperature reduction within canyon was up to 11.3 °C and reached 9.1 °C on average. In contrast, in hot-humid climate of Hong Kong: such reduction was up to 8.4 °C and reached 6.9 °C on average. In Singapore, [Tan et al. \(2014\)](#) measured air temperature reduction of up to 1.1 °C at 1.5 m from green wall while [Hien et al. \(2009\)](#) performed a series of computer simulations to study the effect of greenery coverage on vertical walls on neighborhood's air temperature. When compared with bare facade, the scenarios with 100% facade greenery coverage could lower the air temperature by maximum and average of 1 °C and 0.3 °C, respectively. Also, [Hien et al. \(2010\)](#) measured the effect of eight different vertical greenery façades on ambient air temperature at different distances. The results revealed that the highest reduction in ambient air temperature was 3.3 °C at 0.15m; and was 1.3 °C at 0.6 m away from the walls. Meanwhile, [De Jesus et al. \(2017\)](#) conducted experiments revealed that the reduction in air temperature was 2.5 °C–2.9 °C when compared the effect of green wall to bare wall in the Mediterranean climate of Spain.

In terms of surface temperature, [Yin et al. \(2017\)](#) found up to 8 °C reduction in an experimental study in the hot-humid climate of Nanjing. In a similar climate, [Hien et al. \(2010\)](#) and [Ong et al. \(2000\)](#) have measured a surface temperature reduction of up to 11.6 °C in Singapore. In a Mediterranean climate of Greece, [Eumorfopoulou and Kontoleon's \(2009\)](#) simulation shows exterior surface temperature reduction of an east wall due to plant-covered façade by 1.9 °C–8.3 °C, and 5.7 °C on average while the interior surface temperature of that east wall due to plant-covered façade was from only 0.4 °C–1.6 °C, and 0.9 °C on average. Recently, [Cuce \(2017\)](#) measured reduction in surface temperature of up to 6.1 °C and 4 °C under sunny and cloudy days, respectively between a bare and green wall.

While the effect of vertical greening on fundamental climatic parameters have received enormous research attention as reported above, relatively little progress have been made in addressing its effect on either indoor or outdoor thermal comfort until recently ([Tan et al., 2014](#); [Hien et al., 2009](#)). In these few studies, the mean radiant temperature (MRT) was often used to characterize the thermal comfort condition. [Hien et al. \(2009\)](#) performed a numerical study on the effect of vertical greenery system on indoor mean radiant temperature (MRT), their study found 10.4 °C MRT reduction in a room with 100% outdoor facade greenery coverage assuming no windows on the walls. In contrast, the same study performed similar simulations in which the building has both glass and concrete surface at a window-to-wall ratio of 2:3 and found a difference of just 1.3 °C between a building with 0% and 100% facade greenery coverage. Outdoors, [Tan et al. \(2014\)](#) found MRT was 10.9–12.9 °C higher at 0.5 m of a bare wall relative to green wall due to higher exposure of the former to more intense direct solar

radiation. They also found a “distance to wall” disparity and the positive effect was evident up to 1 m away from the wall.

In summary, most of these previous studies focused on the effect of vertical greening on reduction in ambient air temperature, a few on reductions in surface temperatures and very few on thermal comfort. In fact, these studies are limited to local or building scale while just one reported on neighborhood scale which is of interest in the present study. Therefore, the present study aims at investigating the effect of vertical greenery on thermal comfort and air cooling via its effect on ambient facade surface energy fluxes and air temperature in the typical urban neighborhood of Hong Kong which is a high-density city situated along the coastline of South East China (22°15'N, 114°10'E) with an average altitude of 8m. During her summer months (May to September), Hong Kong experiences a hot-humid sub-tropical climate with average temperature is around 28.5 °C and humidity of 60–95% ([Acero and Herranz-Pascual, 2015](#)).

2. Methodology

The methodological framework for this study is presented in [Fig. 1](#). Mainly, it is made up of two broad phases: Phase 1 (in blue) comprises of field measurement campaign, numerical modelling of measurement site and model validation while Phase 2 (in red) is mainly a parametric study which is composed of several case scenarios of combination of urban density and greening details. Following is detailed description of the adopted methodology for each phase.

2.1. Field measurement campaign

This was conducted at the Hong Kong Government's Energy and Mechanical Service Department (EMSD)'s south-facing vertical greening facility (see [Fig. 2\(a–d\)](#)) during winter and summer seasons of 2017. Interestingly, the green wall composed of plants of four aesthetically interplanted species (*Asparagus cochinchinensis*, *Phyllanthus myrtifolius*, *Chlorophytum comosum*, *Peperomia obtusifolia*) is placed side by side bare (concrete) wall and are of similar height (8 m) (see [Fig. 2\(c\)](#)), making it a perfect site for comparative experimental study. Alongside the ambient meteorological condition monitored using TESTO 480 (see reference for technical details) (n.d.), we are mainly interested in quantifying the contribution of building facades to thermal environment, hence, we also measured facade surface temperature using FLIR's SC 660 thermal camera (FLIR, n.d.) and six-directional radiative fluxes by Kipp & Zonen, CNR4 radiometers (see reference for technical details) ([Kipp and Zonen, n.d.](#)) with focus on the wall-emitted fluxes. The measurement campaign lasted for four days consisting of two winter days (from 11:00 to 17:00 on 28 Feb 2017; from 9:00 to 17:00 on 1 Mar 2017) and two summer days (from 9:00 to 17:00 on 29 Jun 2017; from 9:00 to 16:00 on 13 Jul 2017). This schedule was targeted at understanding the seasonal variation of considered parameters under different sky conditions. All instruments except the FLIR thermal camera were mounted on a tripod (see [Fig. 2\(c\)](#)) placed at 1.5 m away from the walls and at 1.5 m height and logging at 10 s intervals. As we have only one set of the instruments, we alternate between the walls at

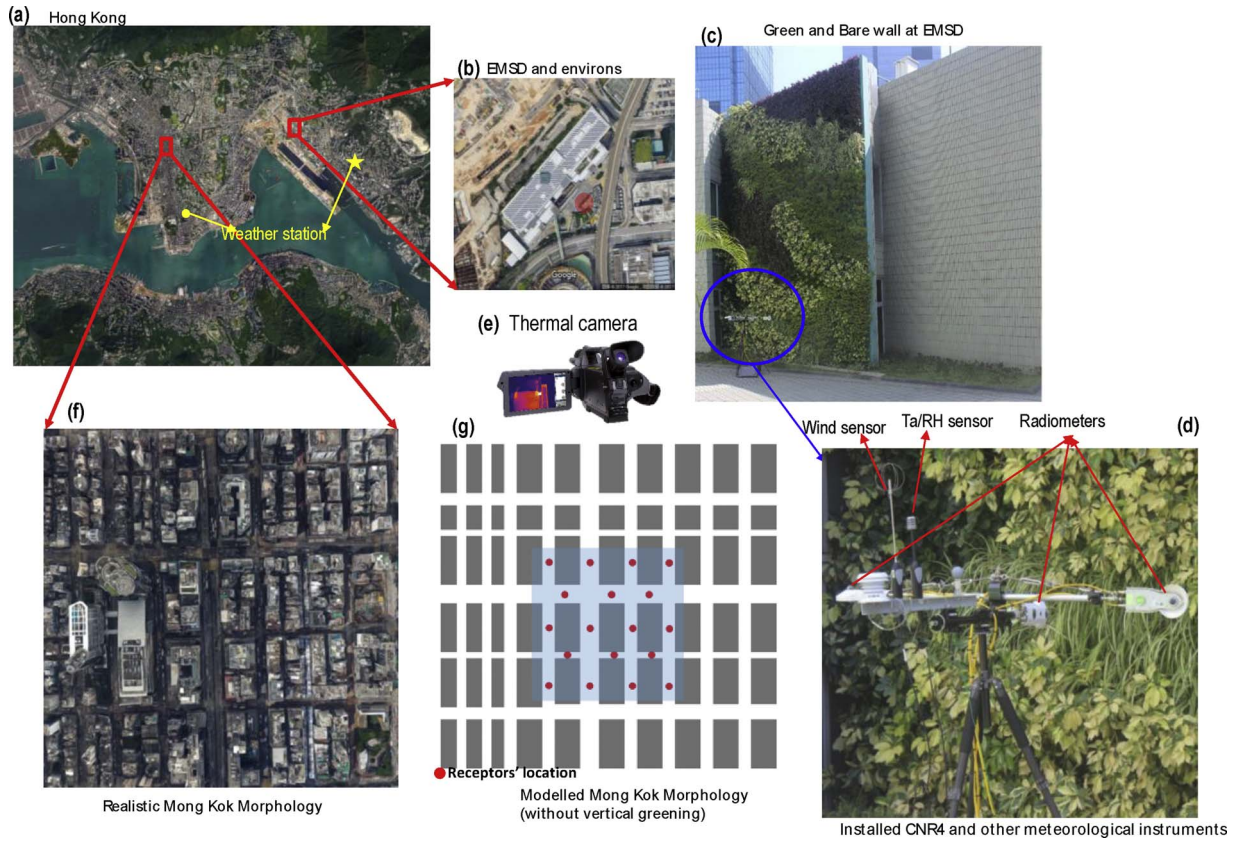


Fig. 2. Field measurement and parametric study sites/model. (a) Map showing the Kowloon Peninsula of Hong Kong (b) zoomed layout of the measurement site i.e. EMSD, (c) Vertical greening facility of EMSD, (d) Instrument setup for measurement (e) thermal camera used for measuring facade surface temperature (f) Zoomed Mong Kok area for parametric study (g) Modelled Mong Kok morphology showing location of receptors evenly distributed in the inner core of the study domain.

15-min intervals during the measuring period. The averaged 5-min median value (i.e. data at the middle of each 15-min intervals) was extracted and analyzed to represent the effect of corresponding surfaces in that interval. Thermal image of the walls were taken each hour and spot data for each wall was extracted and analyzed.

To objectively assess the level of thermal comfort in a space, thermal indices are commonly derived from four fundamental physical parameters: air temperature (Ta), relative humidity (RH), air velocity (v), and mean radiant temperature (MRT) with the latter being the most important for the widely used thermal indices like Physiological Equivalent Temperature (PET)¹ (Höppe, 1999) used in this study. The index selection was due to its consideration of radiation fluxes (i.e. MRT) which significantly depends on the sum of long-wave and short-wave radiant energy fluxes approaching to a human body from all possible directions and wavelengths in the built environment (Tan et al., 2013) and can be estimated using the integral radiation method (Thorsson et al., 2007) presented in Appendix A.

Based on the experimental setup, radiant energy of all directions are similar when around the green and bare walls except for the emitted longwave from that of the walls. Therefore, to delineate the effect of only wall surface type or material on pedestrian thermal comfort, the use of Long-wave Mean Radiant Temperature, LMRT, has been introduced (Jänicke and Meier, 2015). It represents the effective mean surface temperature of surrounding objects in an environment that a human body is exposed to. LMRT can also be regarded as a degenerated version of MRT by only taking account of long-wave radiant fluxes rather than long-wave and short-wave radiant fluxes from all directions.

¹ PET is the air temperature at which, in a typical indoor setting (without wind and solar radiation), the heat budget of the human body is balanced with the same core and skin temperature as under the complex outdoor conditions to be assessed.

By setting the mean radiant flux density S_{str} as the weighted sum of only long-wave radiant fluxes (W.SumL), LMRT would be obtained (Eqs. (1) and (2))

$$S_{str} = W \cdot SumL = \epsilon_p L_i, i = \text{from the wall} \quad (1)$$

thus

$$LMRT = (S_{str}/\epsilon_p \sigma)^{0.25} - 273.15 \quad (2)$$

Where

ϵ_p = the emissivity of human body. According to Kirchhoff's law ϵ_p is equal to the absorption coefficient for long-wave radiation (standard value 0.97)

S_{str} = as the weighted sum of only long-wave radiant fluxes

L_i = directional long-wave radiant fluxes from the wall

σ = the Stefan-Boltzmann constant ($5.67 \times 10^{-8} \text{ W m}^{-2} \text{ K}^{-4}$)

2.2. Numerical modelling of measurement site

Prior to the parametric study (Phase 2 of this study), there is need to assess the performance of the employed model, ENVI-met. To achieve this, we constructed a model of our measurement site (EMSD) and environs i.e. buildings, vertical greening and other physical features in the model. Simulated and measured parameters were compared and statistically evaluated. Before discussing the model setup, we give a brief description of the ENVI-met model below:

2.2.1. Description of ENVI-met model

ENVI-met V4 (hereafter, ENVI-met) (Huttner and Bruse, 2009) is a three-dimensional (3D) non-hydrostatic, micro-climatological, and computational fluid dynamics model which uses the standard $k - \epsilon$ turbulence model in closing the Reynold Average Navier-Stokes (RANS)

equations. The model possesses ability to simulate surface-plant-atmosphere interactions in complex urban environment composed of buildings of different shapes, height and materials; road or surface of different materials and vegetation of different configuration. The model simulates at fine (spatial 0.5–10 m) and temporal (up to 10 s) resolution grid making analyses of small-scale interactions between individual buildings, surfaces and plants achievable. In the model, plants (i.e. trees and grasses) are not only treated as permeable media to wind flow and solar insolation, but are actually biological bodies which interact with the surrounding environment by energy absorption and evapotranspiration. In addition, trees are modelled as three dimensional (3D) complex element using an appended software, 'ALBERO'. To achieve this, vertical and horizontal profile of Leaf Area Density (LAD) and horizontal canopy structure must be foreknown. On the other hand, the developer recommends simple one-dimensional (1D) plant commonly referred to as 'simple 1D plant' for the representation of grasses and also suggested it for green roof (extensive) and green wall related research. Currently, ENVI-met doesn't have a comprehensive green wall or green facade module, an indirect method suggested by the developer is to append 'simple 1D plant' on the grid before the corresponding wall to achieve shading from direct sunlight thereby cooling the wall surface, reducing emitted longwave radiation and improving the overall thermal environment. Previous studies (Jänicke and Meier, 2015; Zölch et al., 2016) have adopted this technique and the present study did likewise.

2.3. Model validation: simulation setup for measurement site

The model of EMSD was developed using buildings' and streets' layout and dimension information of the neighborhood obtained from the Hong Kong Planning department database. The simulation domain is 200 m × 160 m × 90 m with a horizontal (Δx and Δy) and vertical (Δz) grid of 2 m and 3m, respectively. The building (including podium) height in our selected domain ranges between 8–52 m and were all assumed to be made of concrete while the streets are mainly made of concrete overlaid with asphalt. As earlier mentioned, we mimicked green wall in ENVI-met by placing simple 1D plant (i.e. grass) of leaf area density (LAD) of 2 m²/m³ on the grid cell before the corresponding wall. To initialize the simulation, meteorological record (hourly air temperature and relative humidity, prevailing wind speed and direction) of each of the measuring day was obtained from the nearby Tseung Kwan O weather station (see Fig. 2(a)) and forced as boundary condition for the corresponding day's simulation. Summary of all input parameters and values for the validation's simulation exercise can be found in Table 1.

2.4. Parametric study: model setup and scenario development

With the successful validation (results presented later) of the ENVI-met model, the research now focused on the parametric study (Phase 2 of this study). Here, several parametric scenarios was developed to understand the effect of urban density, green facade ratio and greened orientation on air cooling and thermal comfort in the neighborhood. In the subsections below, the model setup, configuration and initialization input values for the study are fully discussed.

2.4.1. Setup of parametric study

The parametric study was based on a typical urban morphology of Hong Kong, specifically using Mong Kok district as case study (as shown in Fig. 2(a) and (d)). This district lies in the core urban area and has the highest population density in the world of 130,000 inhabitants per km² with regular street layout and dense building blocks (Ng et al., 2012). Generally, three parameters were amalgamated to form 24 variances of simulation scenarios:

1) Building and road information: Similar to the setup of our previous

Table 1

Summary of input, test parameters and corresponding values for validation simulation.

Parameter	Definition	Input value
Meteorological conditions ^a	Initial air temperature (°C)	Hourly profile for each day
	Relative Humidity (%)	Hourly profile for each day
	Inflow direction	20° (28th Feb.), 220° (29th June and 13th July)
	Wind speed at 10 m (m/s)	3.1 (28th Feb.), 4.2 (29th June), 3.21 (13th July)
	Soil temperature (°C)	20
Building information	Building and wall height (m)	8–52
	Bare wall, road and roof albedo	0.3
Green wall	Plant type	Grass i.e. simple 1D plant
	Leaf Area Density (m ² /m ³)	2
	Plant albedo	0.32
	Height of wall (m)	8

^a Obtained from the nearby Tseung Kwan O Observatory (see Fig. 2(a)).

study on this district (Ng et al., 2012), real morphological (of buildings and roads especially) were simplified to developed a generic layout plan. Building sizes in the layout were aggregated as blocks, ranging in size from 20 × 40 m², 20 × 80 m², and 80 × 80 m² while the streets' widths were 10, 15, 20, and 30 m. In terms of building height, it was first set to 60 m, representing the realistic average building height of the area (Case 'H' series) which implies a characteristic Hong Kong's morphology of aspect ratio, AR = 2–6 (building-height-to-street-width). With this average building height, two building forms were studied: Without and with podium (compare buildings in Fig. 6(a) and (b)). The latter is now typical of new buildings where towers (40 m in our case) is structurally situated on 20 m podiums. To investigate the influence of urban density on the cooling potentials and thermal comfort improvement of façade greening, two other building heights (without podium) of 30 m (medium density, case 'M' series) and 10 m (low density, case 'L' series) were simulated and compared with their case 'H' series counterpart. Building materials defined in the model were similar in all simulated cases so as to focus on the urban form based comparison only. The overall domain of the model was 500 × 500 × 150 with a horizontal grid size of 5 × 5 m², while the vertical grid size was also set to 3 m.

2) Greened Orientation (GO) and Greened Façade Ratio (GFR): Coupled with the above, five façade greening scenario were considered based on the greened orientation: All four facades (4F), East-West only (EW), East only (E), West only (W) and North-South only (NS) on the regular buildings (no podium) of high, medium and low densities top-down (see Table 3). We further parameterize this based on the ratio of total greened façade surface area to total façade surface area, referred to Greened Façade Ratio (GFR). Therefore, the GFR of greened orientation- 4F, EW, E, W and NS is 100%, 67%, 34%, 34% and 33%, respectively. Furthermore, for the case 'H' cases (with podium), we tested different realistic and implementable façade greening option with the minimal GFR of ~30% (see Table 3 for details). Overall, a total of twenty-four (24) study cases were tested as summarized in Table 3 and Fig. 6 (Case H only). The study cases were designed to determine the location (i.e. orientation and nearness to surface) and amount (i.e. greened coverage) of greening necessary for efficient cooling and thermal comfort improvement per urban density.

2.4.2. Parametric models initialization

To initialize our model, hourly air temperature and relative

Table 2
Summary of input, test parameters and corresponding values for parametric study.

Parameter	Definition	Base cases value
Meteorological conditions ^a	Initial air temperature (°C)	Typical summer profile (see Fig. S1)
	Relative Humidity (%)	Typical summer profile (see Fig. S1)
	Inflow direction (°)	220
	Wind speed at 10 m (m/s)	3
	Soil temperature (°C)	20
Building morphology	Building height	10, 30 and 60
	Road Width (m)	10–30
	Bare Wall, road and roof albedo	0.3
Green wall	Plant type	Grass i.e. simple 1D plant
	Height	Same as building height
	Plant albedo	0.32
	Leaf Area Density (m ² /m ³)	2

^a Obtained from Hong Kong Observatory (HKO) (see Fig. 2(a)).

humidity of a typical summer day (see Fig. S1) were forced at the model boundary using the ‘model forcing’ approach. This technique ensures better accuracy by reducing error caused by boundary conditions. On this day, the minimum and maximum temperature was 26.2 °C and 33.7 °C, respectively while the relative humidity was 60–89%. Furthermore, wind speed at 10 m above the ground level (reference height) was set to 3 m/s with South-Westerly flow direction (220°) to represent a typical summer flow in Hong Kong. Wall, road and roof albedo were both set to 0.3, initial soil temperature was set to 20 °C while the green wall was represented by placing simple 1D plant (i.e. grass) of leaf area density (LAD) of 2 m²/m³ on the grid cell before the corresponding wall. Simulation was performed under a cloud-free sky condition to typify a sunny summer day for 24 h (06:00–05:00) while data of 12:00/15:00 and 23:00 were analyzed as daytime and night time conditions, respectively (the previous data were taken as spin up). Summary of all input parameters and values for the parametric study

Table 3
Simulated scenarios in the parametric study.

Urban density	Case code	Green wall details	GFR (%)
Low (BH = 10 m) Case ‘L’ series	L0	Bare wall (No greening)	0
	L100	All four facades greened top-down	100
	L67	East-West only greened top-down	67
	L30-A	East only greened top-down	33
	L30-B	West only greened top-down	33
	L30-C	North-South only greened top-down	34
Medium (BH = 30 m) Case ‘M’ series	M0	Bare wall (No greening)	0
	M100	All four facades greened top-down	100
	M67	East-West only greened top-down	67
	M30-A	East only greened top-down	33
	M30-B	West only greened top-down	33
	M30-C	North-South only greened top-down	34
High (BH = 60 m) Case ‘H’ series	H0	Bare wall (No greening)	0
	H100	All four facades greened top-down	100
	H67	East-West only greened top-down	67
	H30-A	East only greened top-down	33
	H30-B	West only greened top-down	33
	H30-C	North-South only greened top-down	34
	H30-D	Only East-West podium (20 m high) greened	31
	H30-E	Podium (20 m high) and tower (40 m high) greened on North-South orientations only	28
	H30-F	30 m tall greenery on East-West tower only ^a	32
	H30-G	10 m and 8 m tall greenery on podium and tower, respectively on all orientations	33
	H30-H	8 m and 10 m tall greenery on podium and tower, respectively on all orientations	31
H30-I	Only East-West podium (10 m high) and tower (14m) greened	30	

BH = Building height; GFR = Greened façade ratio.

can be found in Table 2. After the simulations, data extracted at each of the eighteen (18) receptors (see Fig. 2(e)) located in the inner part of neighborhood at 15:00 (for daytime) and 23:00 (for nighttime) were analyzed and discussed.

3. Results and discussion

3.1. Experiment results: hourly variation of LMRT

Comparison of hourly LMRT from both walls, in different seasons and measurement days is depicted in Fig. 3. The measured values of long-wave radiant fluxes (see Fig. 4) were converted into radiant temperature i.e. LMRT (Eq. (1) and (2)). As expected there is a huge deviation between the longwave radiant fluxes and consequently LMRT of winter and summer seasons. This can be attributed to higher solar altitude and intensity in the summer than winter as observed in our result (see Fig. 4) where the direct shortwave radiation was between 156 and 515 W/m² and 62–883 W/m² in winter and summer, respectively. This resulted in ~10 °C difference in LMRT between the seasons irrespective of the facade surface type. In terms of difference between wall surfaces, our results shows that the bare (concrete) significantly emitted more long-wave radiant fluxes than its green counterpart particularly under direct solar radiation and irrespective of seasons. In general, minimum and maximum difference of 0.3–0.8 °C (before noon) and 2.0–2.5 °C (14:00–15:00), respectively was found between the two walls in both winter and summer seasons. In summary, we used Analysis of Variance (ANOVA) to investigate the effect of surface (set as treatment factor) and time (set as block factor introduced to represent the combined effect of all other environmental factors e.g. solar radiation and cloud amount at different times) on long-wave fluxes (and LMRT) on each measurement day. Results (see Tables S1–S4 in supplementary file) showed the null hypothesis of equality on the effect of facade surface on long-wave fluxes (and LMRT) was rejected at 95% confidence interval suggesting a significant difference of the thermal impact of the walls under the same environmental conditions. Besides, the null hypothesis on the relative differences between the walls in summer and winter seasons was also rejected i.e. the relative difference was significantly higher in summer than winter (see Table S5). Hence, further discussion

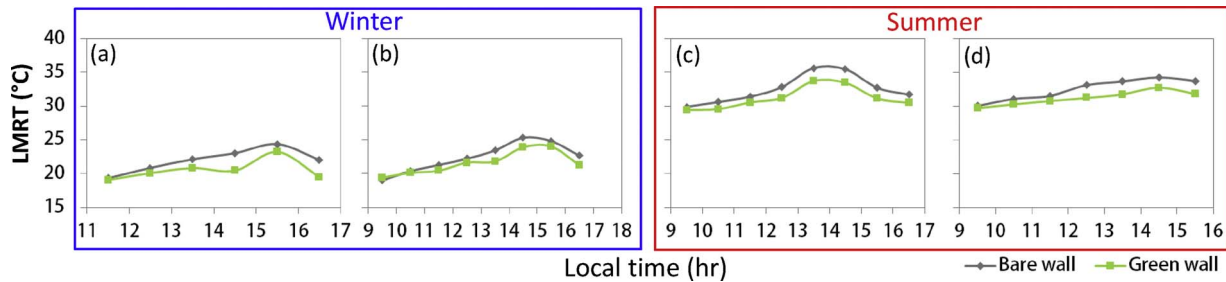


Fig. 3. Radiant temperature or LMRT on during winter ((a) 28 Feb and (b) 01 March) and summer ((c) 29 June and (d) 13 July, 2017) days.

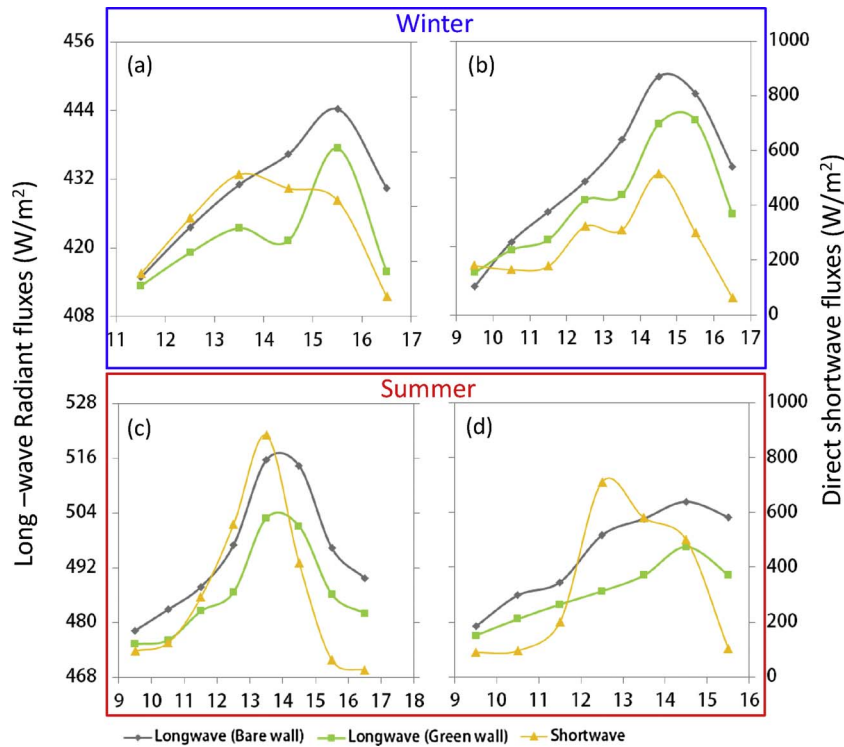


Fig. 4. Hourly variation of measured long-wave and direct shortwave fluxes on during winter ((a) 28 Feb and (b) 01 March) and summer ((c) 29 June and (d) 13 July, 2017) days.

is based on the summer condition due to higher LMRT in this season.

3.2. Comparison between simulated and measurement data

Fig. 5 shows the correlation statistics between simulated and measured wall-emitted longwave radiation (L_w), facade surface temperature (T_{surf}), T_a and RH. Results shows slight underestimation of L_w , T_{surf} and RH at all hours of the day while the T_a was only underestimated during the peak solar hour (12:00–15:00).

Furthermore, quantitative performance statistics with three metrics i.e. coefficient of determination (R^2), Root Mean Square Error (RMSE) and Mean Absolute Percentage Error (MAPE) was calculated and results shown in Table 4. Fair to strong correlation of $R^2 = 0.66$ – 0.70 , 0.60 – 0.74 , 0.89 and 0.76 was found between the two dataset for L_w , T_{surf} , T_a and RH, respectively with a relative low RMSE corresponding to MAPE of 1.1% (for T_a), 14% (for RH), 5.8% (for green wall T_{surf}), 12% (for bare wall T_{surf}) and 7.7% (for bare wall L_w) and 8.5% (for green wall L_w). These results suggest a fair representation of reality by the model as corroborated by validation results from other previous studies who also found strong correlation i.e. $R^2 = 0.79$ – 0.96 and $R^2 = 0.77$ – 0.85 between modelled and measured T_a (Srivani and Hokao, 2013; Müller et al., 2013; Morakinyo et al., 2017; Berardi, 2016; An et al., 2015; Peng and Jim, 2013) and MRT (Lee et al., 2016; Acero

and Herranz-Pascual, 2015), respectively with $< 25\%$ percentage error. Few studies have validated the model for facade related research; Jänicke and Meier (2015) revealed MRT and downward short-wave radiation were reasonably simulated while the model was not able to simulate the effects of facade greening with their applied setting which could be because the authors didn't delineate LMRT from MRT. In a recent study (Paper et al., 2017) on T_{surf} shows $R^2 = 0.96$ – 0.99 and RMSE of 1.03 – 2.13 °C. Basically, the performance of the model hinges on quality of input data. For instance, thermal properties (such as emissivity, thermal conductivity, specific heat capacity, absorption coefficient etc.) of bare wall and green wall (plant albedo and foliage density) material were assumed in our model which could have been better obtained by field measurement where required instruments are available. Secondly, fixed wind condition and static cloud-free condition was assumed which may be responsible for the overestimation of incoming solar radiation during the morning and the afternoon (Acero and Arrizabalaga, 2016). Nevertheless, based on satisfactory performance statistics obtained from our model validation results, especially those related to facade thermal properties and resulting parameters i.e. facade temperature, longwave radiation and radiant temperature, it could be fair to say that ENVI-met is reasonably suitable for simulation of micro-climate and facade related parameters and therefore adopted for the parametric study using the tested and validated setting.

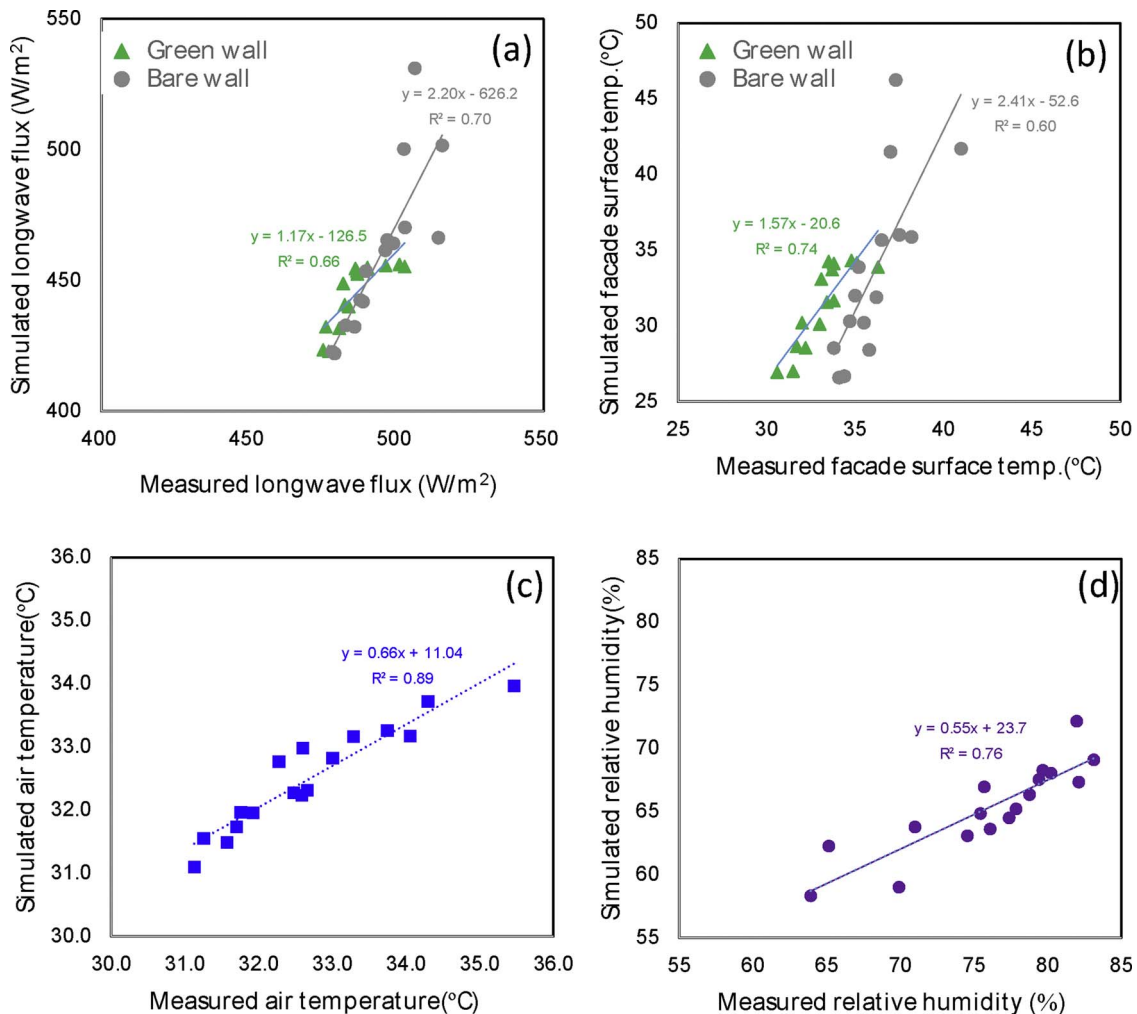


Fig. 5. Comparison of simulated and measured (a) emitted longwave radiation from the facades, (b) facade surface temperature (c) ambient air temperature and (d) relative humidity.

3.3. Results from parametric study: cooling effect of vertical greening in high density setting

The response of diurnal and nocturnal air temperature to greened facade ratio, greened orientation and urban density is discussed in this section using outputs from our ENVI-met simulation. Spatial distribution of the temperature difference ($\Delta T_a = T_{a(\text{greenwall})} - T_{a(\text{barewall})}$) for daytime and nighttime is presented in Figs. S2 and S3, respectively. Further discussions are based on data extracted and analyzed at each of the eighteen (18) receptors (see Fig. 2(e)) located in the inner part of neighborhood at 15:00 (for daytime) and 23:00 (for nighttime). The $\Delta T_a = T_{a(\text{greenwall})} - T_{a(\text{barewall})}$ at each receptor was plotted as in Fig. 7. We first discuss result of the typical high-density setting of Hong Kong (building height = 60 m) while the effect on other urban densities follows subsequently.

If implemented in the high-density setting of Mong Kok and surrounding districts, facade greening could result in daytime temperature change ($\Delta T_a = T_{a(\text{greenwall})} - T_{a(\text{barewall})}$), presented as [Min, Max] ranging between $[-3.2, -1.4]$ °C if all the four facades (100% GFR) are greened. When only East-West (67% GFR), East (33% GFR), West (33% GFR), and North-South (34% GFR) is or are greened, $\Delta T_a = [-2.9, -0.9]$ °C, $[-0.5, 0.2]$ °C, $[-0.9, -0.2]$ °C, and $[-1.0, 0.4]$ °C, respectively. With the more realistic options i.e. H30-D, H30-E, H30-F, H30-G, H30-H, H30-I yields a daytime ΔT_a of $[-0.5, 0.1]$ °C, $[-0.8, 0.2]$ °C, $[-0.3, 0.2]$ °C, $[-1.4, -0.3]$ °C, $[-1.3, -0.3]$ °C, and $[-0.8, -0.1]$ °C, respectively. The presented results is however lower than that observed in another simulation study by Alexandri and Jones

(2008) who found mean temperature decrease of up to ~ 3.0 °C with EW facade greenery systems in an urban canyon of Hong Kong as compared to ~ 0.5 °C obtained with similar greened orientation in our study. Also, in another simulation study (Hien et al., 2009) in a similar climate of Singapore, 100% GFR of buildings in an estate yielded 1 °C maximum reduction. These discrepancies can be attributed to differences in model physics, model setup, thermal properties of building materials and representation of plants in their models as compared to ours. Besides, these studies are wholly simulation studies with no measurement data for validation, in contrast to the present study.

Implementation of green facades is also beneficial for night-time temperature reduction. Our simulation results reveals nighttime $\Delta T_a = [-5.0, -3.4]$ °C, $[-2.8, -0.8]$ °C, $[-1.3, -0.5]$ °C, $[-1.6, -0.4]$ °C, and $[-1.6, -0.2]$ °C when four facades (100% GFR), East-West (67% GFR), East (33% GFR), West (33% GFR), and North-South (34% GFR) is/are greened, respectively. With the more realistic options i.e. H30-D, H30-E, H30-F, H30-G, H30-H, and H30-I nighttime ΔT_a of $[-0.8, -0.4]$ °C, $[-0.9, -0.3]$ °C, $[-0.9, -0.2]$ °C, $[-1.2, -0.5]$ °C, $[-1.1, -0.4]$ °C, and $[-0.9, -0.4]$ °C was realized, respectively. The nighttime results show potential mitigation measures to the urban heat island menace which is prominent in high-density areas. For instance, at the Hong Kong Observatory headquarter station which is very close to the neighborhood in consideration, Wang et al. (2016) revealed 3.8 °C–4.8 °C urban heat island intensity. Implementation of 30% GFR in this area could help reduce this problem by at least ~ 1 °C. This is a greenery strategy that could be harnessed in this area where tree-planting is least beneficial for daytime cooling as the shadow-casting

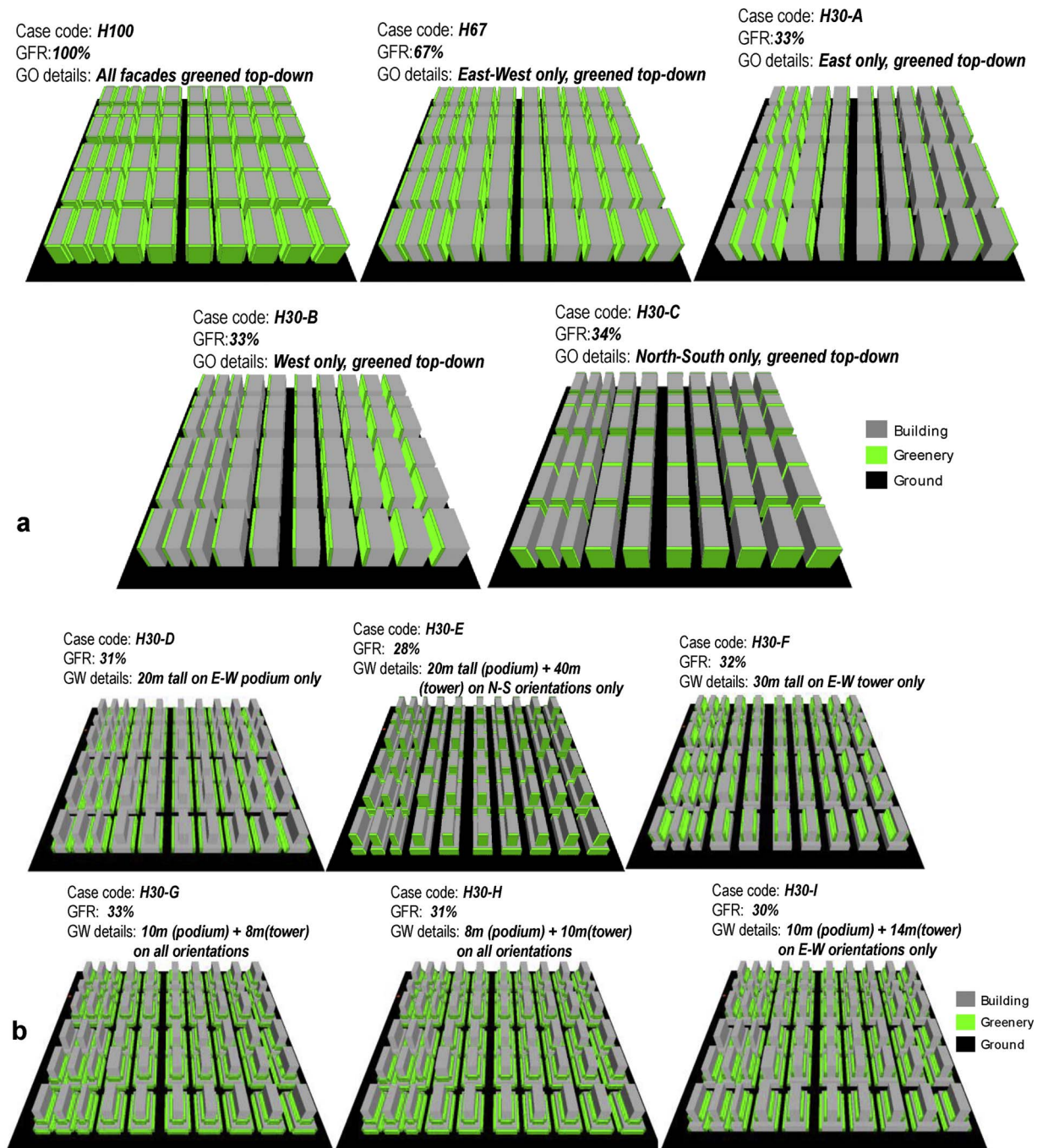


Fig. 6. (a) Simulated scenario in the parametric study [Regular building form (no podium), High density scenario, similar for other urban density with changes in height]. (b) Simulated scenario with realistic Hong Kong's building form and implementable façade greening options.

effect outweighs it (Morakinyo et al., 2017; Morakinyo and Lam, 2016). Moreover, during nighttime, tree shading reduces the escapement of longwave radiation which then warms up the area as previous reported (Morakinyo et al., 2017). Hence, green facades give multiple thermal benefit of daytime, and nighttime air cooling and thermal comfort improvement (as will be discussed later).

3.3.1. Effect of urban density on cooling effect of green facade

The magnitude of the ΔT_a at both nighttime and daytime is dependent on greenery orientation, urban density (or average building height) and GFR. In line with the Hong Kong Government's initiative "First Sustainable Development Strategy for Hong Kong (2005)" (Tan et al., 2013), building height beyond green spaces is an inevitable planning

parameter contributing to a sustainable urban environment. Therefore, we compared results from two other building heights, 30 m (medium density) and 10 m (low density) with that of 60 m (high-density). Result indicated reducing magnitude of ΔT_a with reducing urban density. For low and medium density setting, daytime ΔT_a ranges between $[-0.7, 1.0]$ °C, and $[-1.7, 0.4]$ °C, respectively against $[-3.2, 0.4]$ °C observed for high-density. For nighttime temperature, no significant difference (± 0.5 °C) was found for low density setting while $[-1.7, 0.4]$ °C and $[-5.0, 0.2]$ °C was observed for medium and high-density setting, respectively. This pattern can be attributed to higher volume of greened facade as the urban density increases. Also, percentage of facade exposed to direct solar heating reduces with increasing urban density. With higher greened surface area and volume, evaporative

Table 4

Quantitative measures of the performance of the ENVI-met model based on measured air temperature, relative humidity, emitted longwave flux and facade temperature (sample size: 17); R²: coefficient of determination, RMSE: root mean square error, MAPE: Mean Absolute Percentage Error.

Parameter	R ²	RMSE	MAPE (%)
Air temperature	0.89	0.5 °C	1.1
Relative Humidity	0.76	11.1%	13.9
Emitted longwave flux			
Bare wall	0.70	40.7 W/m ²	7.7
Green wall	0.66	42.0 W/m ²	8.5
Facade temperature			
Bare wall	0.60	5.1 °C	12.1
Green wall	0.74	2.3 °C	5.8

cooling is greater and sensible heating from the wall surfaces reduces proportionally. These combines to cool down the air of the deeper canyons (or neighborhood) than the shallow ones.

3.3.2. Effect of greened facade ratio and orientation on cooling effect of green facade

In all urban densities, similar pattern of cooling effect variation was observed as driven by the percentage of greened facade i.e. higher GFR results in higher temperature reduction and vice-versa. It is interesting to realize that at neighborhood scale, the orientation of the greened facade is not as important as the greened percentage even though the positioning or placement could be optimized for enhanced benefits.

To put this study into perspective, we investigated how much greened facade is required in reducing daytime and nighttime urban temperature by 1 °C in a hot-humid city like Hong Kong. Therefore, we have plotted the average ΔT_a at pedestrian level against green facade ratio as depicted in Fig. 8. During daytime, results revealed that at least 57% (R² = 0.98) of the facades in the neighborhood domain must be greened for high density setting to achieve this target. While 57% GFR seems unrealistic, four (H30-C, H30-G, H30-H and H30-I) of our realistic options with GFR ~30% could reduce daytime temperature by 0.5–0.8 °C suggesting the innovative placement could augment for high GFR requisite. Furthermore, nearness of green wall to pedestrians was found to enhance temperature reduction as observed with H30-D (31% GFR, greenery on EW podium) and H30-F (32% GFR, greenery on EW tower) where the former gave additional 0.1 °C cooling benefit. It is important to note that the GFR requirement becomes more stringent for other urban densities; for medium density setting, 97% (R² = 0.94) while the target can't be realistically reached in low-density setting.

At nighttime, 30 – 40% (R² = 0.93) and 80% (R² = 0.99) for high and medium density, respectively could potential reduce the intensity of urban heat island by cooling the air by at least 1 °C while the unrealistic 100% facade greening is not even enough at nighttime cooling

in low density setting. Hence, in high-density setting in Hong Kong such Yau Tsim Mong district, not less than 30% vertical greening is realizable and would immensely contribute daytime temperature reduction and urban heat island mitigation apart from other environmental benefits such as energy use reduction and pollution abatement (Alexandri and Jones, 2008; Morakinyo and Lam, 2015; Morakinyo et al., 2016).

3.4. Surface temperature reduction by facade greening

Another parameter often analyzed to estimate the cooling effect of facade greening is surface temperature. The lower the facade temperature, the lower the indoor cooling energy demand and LMRT. In this section, we have quantified the reduction of facade surface ($\Delta T_{\text{surf}} = T_{\text{surf,greened}} - T_{\text{surf,bare}}$) temperature over the four facade orientation when the same or other facades is/are greened. To typify this, we extracted data of the 12:00 mid-day from our ENVI-met simulation output. This is because other measurement studies (discussed earlier) including ours have shown maximum facade cooling effect during the peak solar hour (12:00–15:00). To illustrate this, Figs. 9 and 10 have been presented. The former shows a 3D distribution of ΔT_{surf} in high-density setting as an illustration when different facade(s) is/are greened. Pattern is similar for other urban densities (figure not shown). For discussion, we focused on Fig. 10 which illustrates the extracted ΔT_{surf} for all greened orientation and effect on the bare wall in the three urban densities. Overall, surface temperature reduction varies from 0.3 °C to 16.7 °C depending on the orientation of the greened facade but not significantly related to urban density even though lowest urban density gives high reduction because more portion of the walls are sunlit, the portion reduces as the building height increases. When all the four facades (H100) are greened, depending on the urban density the Eastern facade gives the maximum reduction of 14–16 °C, followed by South-facing facade, 7–11.5 °C, these two facades are more sunlit before noon than the North and West-facing facades which shows 7.5–9 °C. With one or two facades greened (i.e. H67, H30-A, H30-B and H30-C), the greened facades had the most reduction. However, all facades shows slight reduction in any case even when not greened but another is/are greened. It is also important to note that due to higher exposure before noontime, the east-facing facade always show higher ΔT_{surf} than its west-facing counterpart, except when it is not greened. The reverse is the case during the other half of the day when the sun angle changes westwards. Our results are within the range of other experimental studies in the same hot-humid climate. For instance, in Singapore (Hien et al., 2009; Ong et al., 2000) showed up to 11.6 °C surface temperature reduction by green wall (orientation not stated). In another study in Nanjing (Yin et al., 2017), up to 8 °C reduction was found with their studied south-facing green wall.

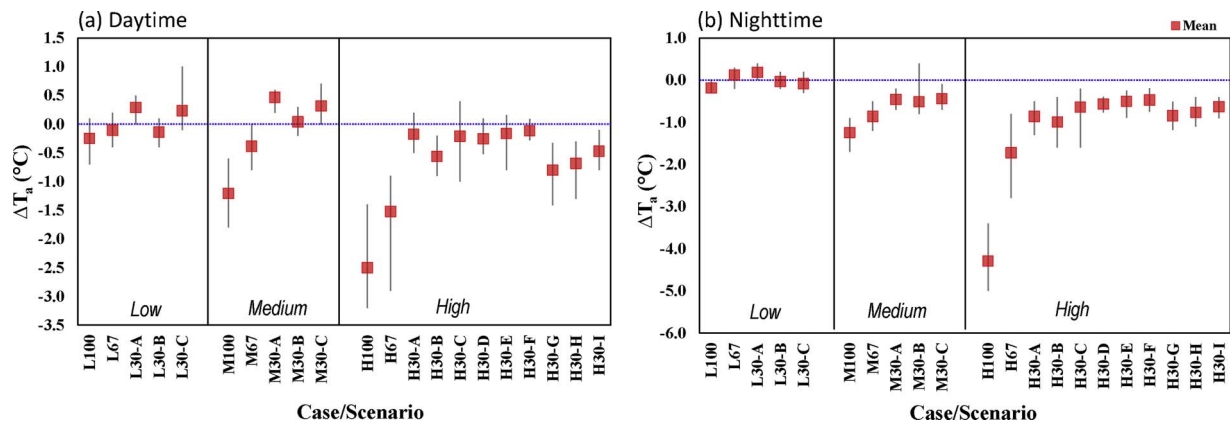


Fig. 7. Variation of cooling effect by facade greening on different orientation and urban density at (a) daytime and (b) Nighttime.

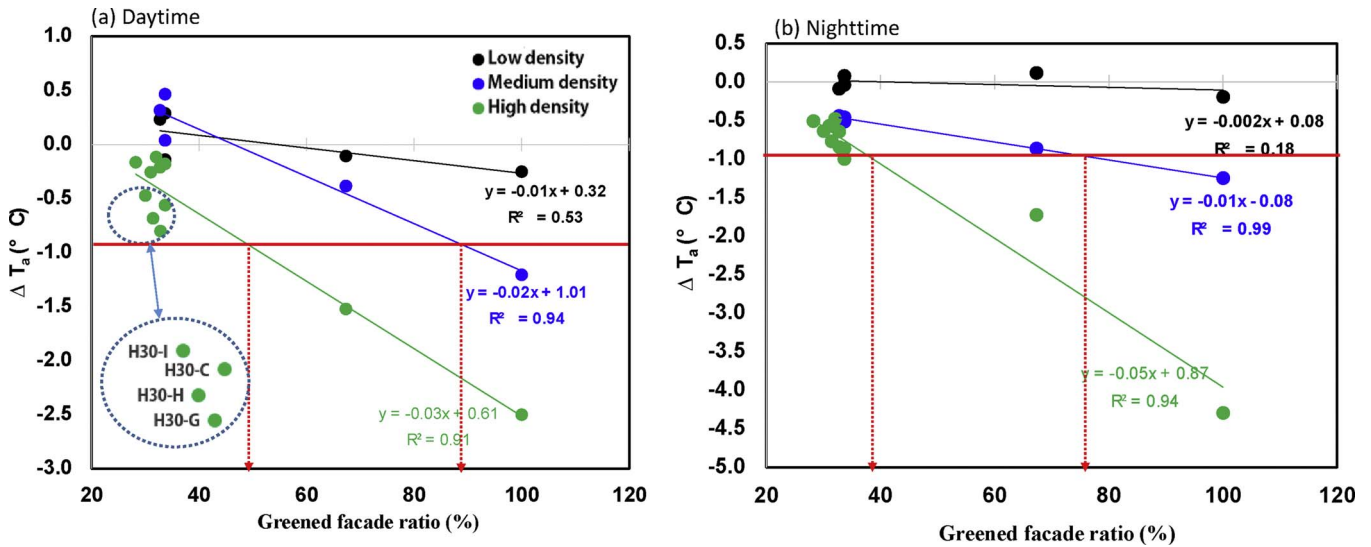


Fig. 8. Relationship between cooling effect by facade greening, urban density and greened facade ratio, (a) daytime and (b) Nighttime.

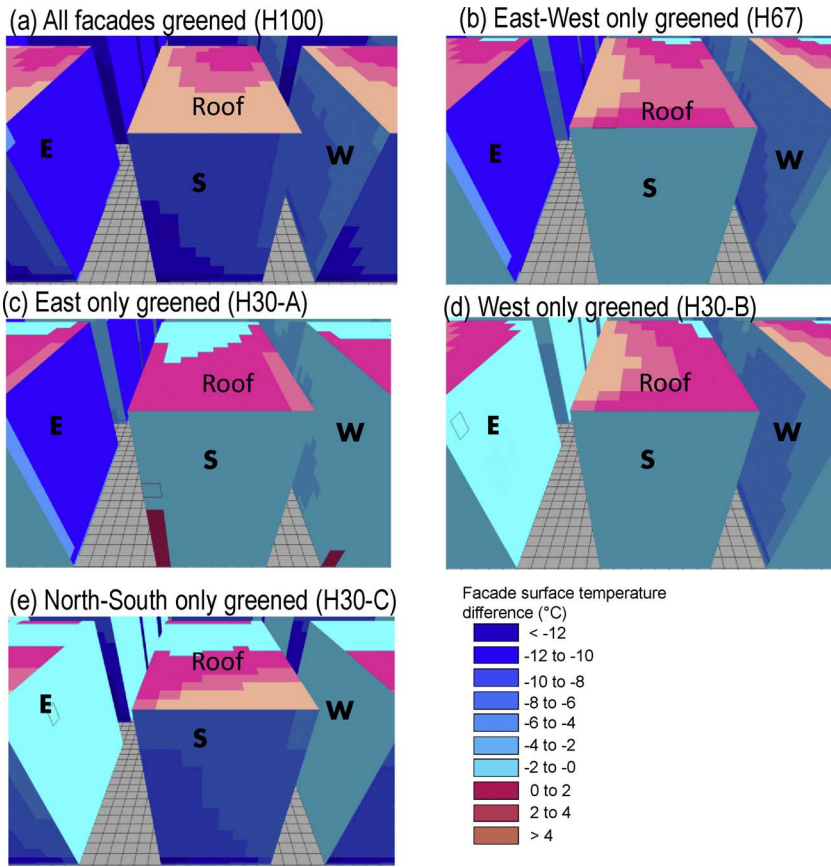


Fig. 9. Distribution of facade surface temperature reduction at midday by facade greening in High-density setting (E: East Facade, S: South Facade; W: West facade. North not accessible at this view angle).

3.5. Thermal comfort improvement with facade greening at neighbourhood scale

3.5.1. Effect of green facade on thermal comfort

As earlier mentioned, thermal comfort in this study was estimated using the Physiological Equivalent Temperature (PET) index, which is a function of air temperature, relative humidity, wind speed and mean radiant temperature. Earlier discussion have extensively shown the role of green facade on air cooling which is a result of the combined effect of surface shading and evaporative cooling potential of vegetation. However, it is important to mention that facade greening is capable of

reducing wind velocity especially near the greened wall (see Fig. S4) which cumulatively led to reduction of ventilation within the domain irrespective of the scenario even though the magnitude varies depending on the GFR, orientation and nearness to pedestrian level. Further discussion in this section will be based on the combined thermal effects i.e. thermal comfort. We present results related to thermal comfort improvement (i.e. $\Delta PET = PET_{(greenwall)} - PET_{(barewall)}$) in [Min, Max] format) of pedestrian if green facade is implemented. Fig. 11(a) shows the daytime ΔPET averagely ranges between $[-4.0, -0.1]^\circ C$, $[-6.0, -2.0]^\circ C$, and $[-10.0, -2.0]^\circ C$ for low, medium and high density setting, respectively regardless of the greened facade ratio and

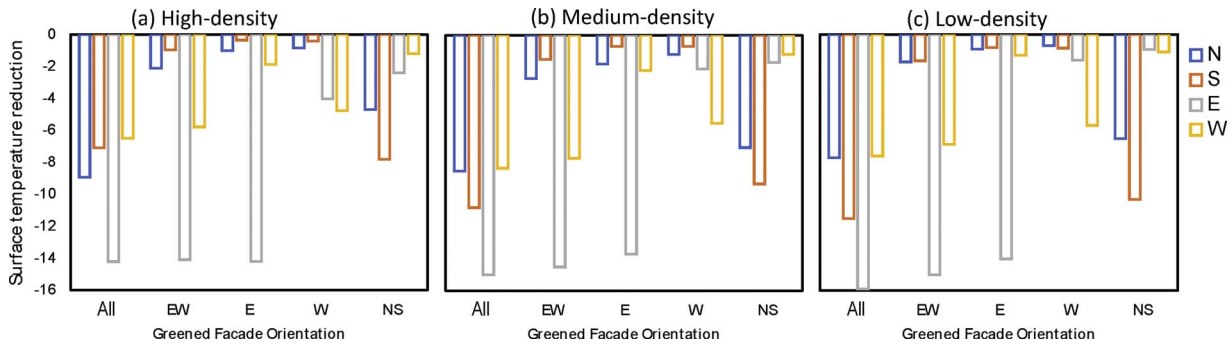


Fig. 10. Average facade surface temperature at midday on each facade relative to the greened facade (s).

orientation. However, at nighttime (Fig. 11(b)), potential improvement of thermal comfort is only plausible in some cases in high-density setting while other setting shows no or negative impact on thermal comfort.

3.5.2. Effect of greened facade ratio and orientation on thermal comfort improvement

The magnitude of Δ PET is mostly dependent on greened facade ratio especially during daytime with $R^2 = 0.67\text{--}0.98$ irrespective of urban density while no notable difference was observed at nighttime although a negative correlation of $R^2 = 0.23\text{--}0.62$ was observed irrespective of urban density. PET reduction at the high-density is least correlated with GFR. Based on Hong Kong’s PET thermal comfort sensation classification (Morakinyo et al., 2017), to improve thermal sensation from one class to the other e.g. from warm to neutral, minimum of Δ PET = 4 °C is required. Therefore we set this as target so as query the percentage of greened facade required to achieve change of thermal sensation per urban density and period. The result is presented in Fig. 12. During daytime, this target is achievable in low-density only with ~100% GFR. However, medium-density setting requires ~60% GFR to reduce the PET by at least 4 °C. The requirement for high-density is much lower, as only less than 30% will help realize the target and with more, the Δ PET is also greater.

4. Planning understanding and recommendations

Based on findings from the parametric study, the following recommendations useful for sustainable urban design and (re)development in Hong Kong are hereby suggested:

- 1 Useful guide for facade greening implementation

Findings from our realistic case studies (H30-D to H30-I) suggest quantity is the most important for neighborhood-wide thermal benefit, the more the overall GFR the better. For instance, case H30-F (28%

GFR) gave the least daytime and nighttime thermal benefit while the most was observed with H30-G (33%). Urban planners, architects and builders can make use of the displayed regression equations (i.e. proposed simple parametric model) on Figs. 8 and 12 determine the greened facade ratio required to effect certain level of urban cooling or thermal comfort improvement, respectively. Note that these equation are dependent on the average building density of a neighborhood and time (either daytime or nighttime). For instance in a compact-high rise neighborhood like Mong Kok, Eq. (3) can be applied for daytime cooling estimation for a proposed greened facade ratio (GFR) as excerpted from Fig. 8(a).

$$\text{Cooling benefit } (\Delta T_a) = -0.03\text{GFR} + 0.61 \tag{3}$$

Also, the greened facade orientation should also be considered, when the same quantity of greenery are applied to East-West and North-South facades, the former will yield better thermal benefits and therefore recommended. Furthermore, we found that the closer the greenery is to the pedestrian the better the obtained benefit. For example, between H30-D(31% GFR) and H30-F(32% GFR), the former yielded additional daytime (vice-versa at night) temperature reduction and thermal comfort benefits even though its GFR is slightly lower. However, where there are constraint on the podium greening, the lower facades of the tower should be greened

- 1 Urban greening recommendations for HK2030 +

In agreement with the recently commissioned HK2030 + Strategic Plan (HK2030 +, 2016) which includes proposal for the introduction of a new “green index” for Hong Kong in replacement of the existing Green Master Plan. We therefore recommend that the new “green index” should include a mix of multiple greening strategies ratios not just tree-planting. This is because several greening solutions can give similar cooling or thermal benefits. For instance, current recommendation of 30% tree coverage ratio is equivalent to 30–50%

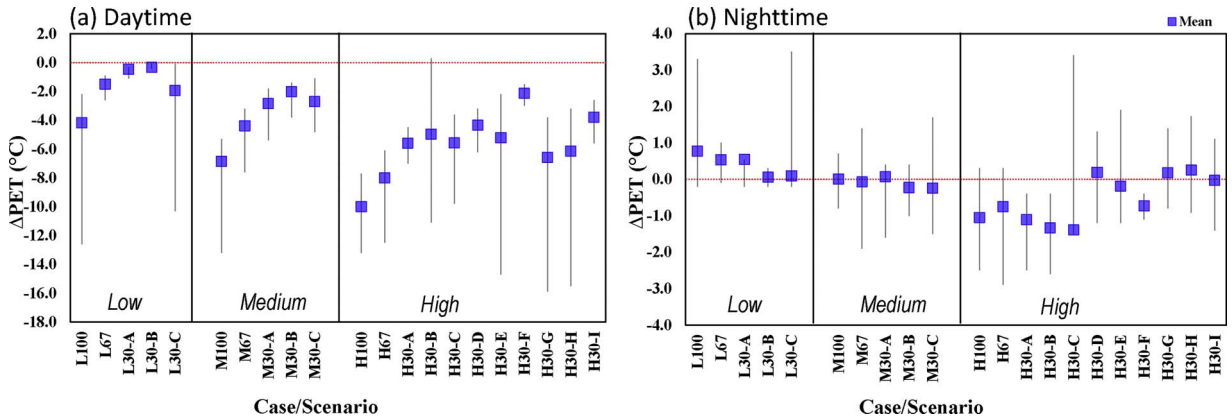


Fig. 11. Variation of thermal comfort improvement (or otherwise) by facade greening on different orientation and urban density at (a) daytime and (b) Nighttime.

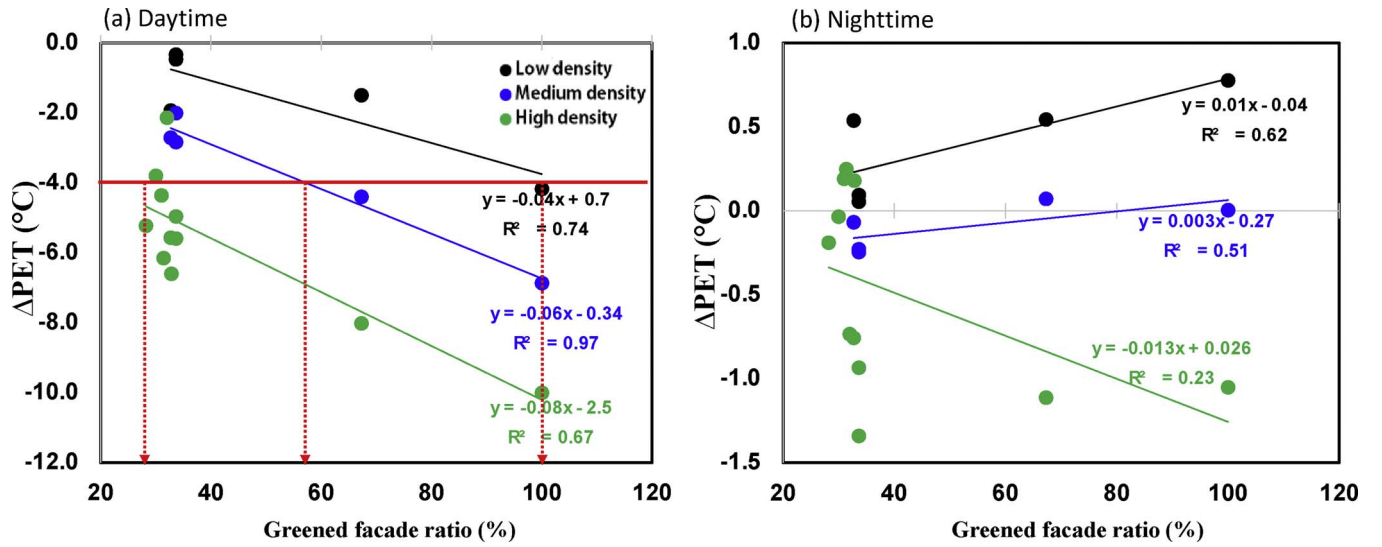


Fig. 12. Relationship between thermal comfort improvement (or otherwise) by facade greening, urban density and greened facade ratio, (a) daytime and (b) Nighttime.

green facade ratio (based on our recent finding) when a $\sim 1^\circ\text{C}$ urban temperature reduction is targeted.

While we have advocated for facade greening, we are not ignorant of the challenges that could hamper its implementation e.g. Cost of installation and maintenance, water demand, and building damage. A major concern specific to Hong Kong is the age of current buildings and their structurally unfit layout for such greening. In fact, it has been projected that there would be about 326,000 private housing units aged 70 or above by 2046 which is nearly 300 times of the building stock of the same age in 2015 (P department, 2016). This suggests that the rejuvenation of dense urban core of Hong Kong (especially Sham Shui Po, Yau Tsim Mong and Kowloon City districts) is imminent and is already one of the key strategic directions of the HK2030+ (P department, 2016). We therefore recommend that future redevelopment should strongly advocate for structural designs that are climate sensitive and greenery (roof and facade) accommodating. We hope that these recommendations if implemented will eventually make Hong Kong a model compact-green city.

5. Conclusion

While innovative incorporation of urban greening strategies into grey infrastructures are key in providing nature-based solution for sustainable and resilient cities, this study have markedly investigated the facade/vertical greening strategy in the subtropical high-density city of Hong Kong. The study used both field measured and simulated dataset to provide scientific evidence on the thermal benefit of facade greening at different urban densities. Using a previously validated

ENVI-met model, we have investigated the quantity of greened facade required to cause significant urban cooling/improved thermal comfort and if the greened orientation(s) matter, since it is impractical to green the all facades of buildings in a neighborhood. Beyond this, we studied the effect of urban density on the potential cooling by facade greening. Results revealed that 30–50% of facade surface area in the high-density urban setting of Hong Kong must be greened to cause $\sim 1^\circ\text{C}$ reduction in both daytime and nighttime air temperature while the same could help improve daytime pedestrian thermal comfort by at least one thermal class. We also found that the greened facade ratio requirement for similar thermal benefit target becomes stricter with reducing urban density while greened facade orientation does not impact the thermal benefit. While green coverage ratio is important, placement at the right location is quite much more imperative to draw their thermal dividends. Furthermore, other strategies such as climate-sensitive urban fabric, improved urban ventilation and rightly placed facade, roof, and ground-level greening should be innovatively combined and applied in urban design planning especially in tropical climates (Morakinyo and Lam, 2016; Lobaccaro and Acero, 2015) to ensure reduction in the thermal load of the urban environment.

Acknowledgements

This work was supported by the General Research Fund from the Research Grants Council of Hong Kong (grant number: 14629516). We are also grateful to EMSD for allowing us conduct field measurement around her vertical greening facility.

Appendix A. Estimation of MRT using integral method

One of the most accurate methods to estimate MRT is by *integral radiation measurement* (Thorsson et al., 2007). By measuring the six individual measurements of the short-wave and long-wave radiant fluxes and multiplying these measured fluxes with corresponding coefficients, a quantity called mean radiant flux density S_{str} of a human body is firstly calculated by Eq. (A1) (VDI, 1998).

$$S_{str} = \alpha_k \sum_{i=1}^6 F_i K_i + \varepsilon_p \sum_{i=1}^6 F_i L_i, \quad i = [1,6] \quad (\text{A1})$$

K_i = directional short-wave radiant fluxes from the i -th direction

L_i = directional long-wave radiant fluxes from the i -th direction

F_i = the view factors between a person and surrounding surfaces

α_k = the absorption coefficient for short-wave fluxes (standard value 0.7)

ε_p = the emissivity of human body. According to Kirchoff's laws ε_p is equal to the absorption coefficient for long-wave radiation (standard value 0.97)

The angular factor (or view factor), F_{ij} , depends on both relative position and orientation of a person (Fanger, 1972). As for a (rotationally

symmetric) standing or walking person, F_i is set to 0.06 for energy fluxes from sky and the ground, and 0.22 for energy fluxes from four cardinal directions (Northerly, Easterly, Southerly, and Westerly) respectively. As for a sphere, F_i is simply set to be one-sixth (i.e. $1/6 \approx 0.167$) for all six directional fluxes. In this study, the mean radiant flux density S_{str} is calculated for a rotationally symmetric standing or walking person and thus the MRT ($^{\circ}\text{C}$) is obtained from Stefan-Boltzmann law:

$$MRT = (S_{str}/\varepsilon_p\sigma)^{0.25} - 273.15 \quad (\text{A2})$$

σ = the Stefan-Boltzmann constant ($5.67 \times 10^{-8} \text{ Wm}^{-2} \text{ K}^{-4}$)

Appendix B. Supplementary data

Supplementary data associated with this article can be found, in the online version, at <http://dx.doi.org/10.1016/j.ufug.2017.11.010>.

References

- Acero, J.A., Arrizabalaga, J., 2016. Evaluating the performance of ENVI-met model in diurnal cycles for different meteorological conditions. *Theor. Appl. Climatol.* 1–15. <http://dx.doi.org/10.1007/s00704-016-1971-y>.
- Acero, J.A., Herranz-Pascual, K., 2015. A comparison of thermal comfort conditions in four urban spaces by means of measurements and modelling techniques. *Build. Environ.* 93, 245–257. <http://dx.doi.org/10.1016/j.buildenv.2015.06.028>.
- Alexandri, E., Jones, P., 2008. Temperature decreases in an urban canyon due to green walls and green roofs in diverse climates. *Build. Environ.* 43, 480–493. <http://dx.doi.org/10.1016/j.buildenv.2006.10.055>.
- An, K.J., Lam, Y.F., Hao, S., Morakinyo, T.E., Furumai, H., 2015. Multi-purpose rainwater harvesting for water resource recovery and the cooling effect. *Water Res.* 86, 116–121. <http://dx.doi.org/10.1016/j.watres.2015.07.040>.
- Berardi, U., 2016. The outdoor microclimate benefits and energy saving resulting from green roofs retrofits. *Energy Build.* 121, 217–229. <http://dx.doi.org/10.1016/j.enbuild.2016.03.021>.
- Bryse, K., Oreskes, N., O'Reilly, J., Oppenheimer, M., 2013. Climate change prediction: erring on the side of least drama? *Glob. Environ. Change* 23, 327–337. <http://dx.doi.org/10.1016/j.gloenvcha.2012.10.008>.
- Cuce, E., 2017. Thermal regulation impact of green walls: an experimental and numerical investigation. *Appl. Energy* 194, 247–254. <http://dx.doi.org/10.1016/j.apenergy.2016.09.079>.
- De Jesus, M.P., Lourenço, J.M., Arce, R.M., Macias, M., 2017. Green façades and in situ measurements of outdoor building thermal behaviour. *Build. Environ.* 119, 11–19. <http://dx.doi.org/10.1016/j.buildenv.2017.03.041>.
- Eumorfopoulou, E.A., Kontoleon, K.J., 2009. Experimental approach to the contribution of plant-covered walls to the thermal behaviour of building envelopes. *Build. Environ.* 44, 1024–1038. <http://dx.doi.org/10.1016/j.buildenv.2008.07.004>.
- Fanger, P.O., 1972. *Thermal comfort: analysis and applications in environmental engineering*. McGraw-Hill, New York.
- FLIR, FLIR thermal image camera, n.d. [http://www.flir.com/uploadedFiles/Thermography_APAC/Products/Product_Literture/SC660_DatasheetAPAC\(1\).pdf](http://www.flir.com/uploadedFiles/Thermography_APAC/Products/Product_Literture/SC660_DatasheetAPAC(1).pdf) (Accessed 8 September 2017).
- Höppe, P., 1999. The physiological equivalent temperature—a universal index for the biometeorological assessment of the thermal environment. *Int. J. Biometeorol.* 43, 71–75. <http://dx.doi.org/10.1007/s004840050118>.
- HK2030+, Hong Kong 2030+ : Towards a Planning Vision and Strategy Transcending 2030, 2016.
- Hien, N., Yong, A., Tan, K., Yok, P., Chung, N., 2009. Energy simulation of vertical greenery systems. *Energy Build.* 41, 1401–1408. <http://dx.doi.org/10.1016/j.enbuild.2009.08.010>.
- Hien, N., Yong, A., Tan, K., Chen, Y., Sekar, K., Yok, P., Chan, D., Chiang, K., Chung, N., 2010. Thermal evaluation of vertical greenery systems for building walls. *Build. Environ.* 45, 663–672. <http://dx.doi.org/10.1016/j.buildenv.2009.08.005>.
- Holm, D., 1989. Thermal improvement by means of leaf cover on external walls—a simulation model. *Energy Build.* 14, 19–30. [http://dx.doi.org/10.1016/0378-7788\(89\)90025-X](http://dx.doi.org/10.1016/0378-7788(89)90025-X).
- Huttner, S., Bruse, M., 2009. Numerical modeling of the urban climate—a preview on ENVI-MET 4.0. *Seventh Int. Conf. Urban Clim.* 1–4.
- Jänicke, F., Meier, M., 2015. Evaluating the effects of façade greening on human bioclimate in a complex urban environment. *Adv. Meteorol.* 2015.
- Kipp and Zonen, CNR4 instruction manual, n.d. http://www.kippzonen.com/Product/85/CNR4-Net-Radiometer#WYqQA_Gv9aS (Accessed 9 August 2017).
- Kontoleon, K.J., Eumorfopoulou, E.A., 2010. The effect of the orientation and proportion of a plant-covered wall layer on the thermal performance of a building zone. *Build. Environ.* 45, 1287–1303. <http://dx.doi.org/10.1016/j.buildenv.2009.11.013>.
- Lee, H., Mayer, H., Chen, L., 2016. Contribution of trees and grasslands to the mitigation of human heat stress in a residential district of Freiburg, Southwest Germany. *Landsc. Urban Plan.* 148, 37–50. <http://dx.doi.org/10.1016/j.landurbplan.2015.12.004>.
- Lin, T.P., Matarzakis, A., Hwang, R.L., 2010. Shading effect on long-term outdoor thermal comfort. *Build. Environ.* 45, 213–221. <http://dx.doi.org/10.1016/j.buildenv.2009.06.002>.
- Lin, T.P., Tsai, K.T., Hwang, R.L., Matarzakis, A., 2012. Quantification of the effect of thermal indices and sky view factor on park attendance. *Landsc. Urban Plan.* 107, 137–146. <http://dx.doi.org/10.1016/j.landurbplan.2012.05.011>.
- Lo, C.P., Luvall, J.C., Quattrochi, D., 1997. Application of high-resolution thermal infrared remote sensing and GIS to assess the urban heat island effect. *Int. J. Remote Sens.* 18, 287–304. <http://dx.doi.org/10.1080/014311697219079>.
- Lobaccaro, G., Acero, J.A., 2015. Comparative analysis of green actions to improve outdoor thermal comfort inside typical urban street canyons. *Urban Clim.* 14, 251–267. <http://dx.doi.org/10.1016/j.uclim.2015.10.002>.
- Müller, N., Kuttler, W., Barlag, A.-B., 2013. Counteracting urban climate change: adaptation measures and their effect on thermal comfort. *Theor. Appl. Climatol.* 115, 243–257. <http://dx.doi.org/10.1007/s00704-013-0890-4>.
- Morakinyo, T.E., Lam, Y.F., 2015. Simulation study of dispersion and removal of particulate matter from traffic by road-side vegetation barrier. *Environ. Sci. Pollut. Res.* 1–14. <http://dx.doi.org/10.1007/s11356-015-5839-y>.
- Morakinyo, T.E., Lam, Y.F., 2016. Simulation study on the impact of tree-configuration, planting pattern and wind condition on street-canyon's micro-climate and thermal comfort. *Build. Environ.* 103, 262–275. <http://dx.doi.org/10.1016/j.buildenv.2016.04.025>.
- Morakinyo, T.E., Lam, Y.F., Hao, S., 2016. Evaluating the role of green infrastructures on near-road pollutant dispersion and removal: modelling and measurement. *J. Environ. Manage.* 182, 595–605. <http://dx.doi.org/10.1016/j.jenvman.2016.07.077>.
- Morakinyo, T.E., Kong, L., Lau, K.K.-L., Yuan, C., Ng, E., 2017. A study on the impact of shadow-cast and tree species on in-canyon and neighborhood's thermal comfort. *Build. Environ.* 115, 1–17. <http://dx.doi.org/10.1016/j.buildenv.2017.01.005>.
- Ng, E., Chen, L., Wang, Y., Yuan, C., 2012. A study on the cooling effects of greening in a high-density city: an experience from Hong Kong. *Build. Environ.* 47, 256–271. <http://dx.doi.org/10.1016/j.buildenv.2011.07.014>.
- Oke, T.R., 1973. City size and the urban heat island. *Atmos. Environ.* 7, 769–779. [http://dx.doi.org/10.1016/0004-6981\(73\)90140-6](http://dx.doi.org/10.1016/0004-6981(73)90140-6). Pergamon Press.
- Ong, L.B., Tiong, L.G., Yu, C., 2000. A survey of the thermal effect of plants on the vertical sides of tall buildings in Singapore. *Proc. PLEA* 495–500.
- P. department and D.B. of H.K.S. Government, Hong Kong 2030+ : Towards a Planning Vision and Strategy Transcending 2030, 2016.
- Paper, C., Gutenberg-universit, H.S.J., Gutenberg-universit, M.B.J., Trees, S., View, U.E., Monde, E., Simon, H., 2017. Evaluation of ENVI-met's multiple-node model and estimation of indoor climate.
- Peng, L.L.H., Jim, C.Y., 2013. Green-roof effects on neighborhood microclimate and human thermal sensation. *Energies* 6, 598–618. <http://dx.doi.org/10.3390/en6020598>.
- Srivani, M., Hokao, K., 2013. Evaluating the cooling effects of greening for improving the outdoor thermal environment at an institutional campus in the summer. *Build. Environ.* 66, 158–172. <http://dx.doi.org/10.1016/j.buildenv.2013.04.012>.
- Stec, W.J., Van Paassen, A.H.C., Maziarz, A., 2005. Modelling the double skin façade with plants. *Energy Build.* 37, 419–427. <http://dx.doi.org/10.1016/j.enbuild.2004.08.008>.
- Susorova, I., Angulo, M., Bahrami, P., Stephens, Brent, 2013. A model of vegetated exterior facades for evaluation of wall thermal performance. *Build. Environ.* 67, 1–13. <http://dx.doi.org/10.1016/j.buildenv.2013.04.027>.
- Takakura, T., 2000. Cooling effect of greenery cover over a building. pp. 2–7.
- Tan, C.L., Wong, N.H., Jusuf, S.K., 2013. Outdoor mean radiant temperature estimation in the tropical urban environment. *Build. Environ.* 64, 118–129. <http://dx.doi.org/10.1016/j.buildenv.2013.03.012>.
- Tan, C.L., Wong, N.H., Jusuf, S.K., 2014. Effects of vertical greenery on mean radiant temperature in the tropical urban environment. *Landsc. Urban Plan.* 127, 52–64. <http://dx.doi.org/10.1016/j.landurbplan.2014.04.005>.
- Testo 480, Testo 480 instruction manual, n.d. https://media.testo.com/media/51/43/180850f3d452/testo-480_Data-Sheet.pdf (Accessed 9 August 2017).
- Thorsson, S., Lindberg, F., Eliasson, I., Holmer, B., 2007. Different methods for estimating the mean radiant temperature in an outdoor urban setting. *Int. J. Climatol.* 27 (14), 1983–1993.
- U.N.F. for Population Activities, U.N.P. Fund, The state of world population, United Nations Fund for Population Activities, 2010.
- VDI (1998). Methods for the human-biometeorological assessment of climate and air quality for urban and regional planning. Part 1: Climate. VDI Guideline 3787, Part 2. Verein Deutscher Ingenieure.
- Wang, W., Zhou, W., Ng, E.Y.Y., Xu, Y., 2016. Urban heat islands in Hong Kong: statistical modeling and trend detection. *Nat. Hazards* 83 (2), 885–907. <http://dx.doi.org/10.1007/s11069-016-2353-6>.
- Wilmers, F., 1990. Effects of vegetation on urban climate and buildings. *Energy Build.* 16,

- 507–514.
- Wong, N.H., Tan, A.Y.K., Tan, P.Y., Wong, N.C., 2009. Energy simulation of vertical greenery systems. *Energy and buildings* 41 (12), 1401–1408.
- Wong, N.H., Tan, K., Chen, Y., Sekar, K., Tan, Y., Chan, D., Wong, N.C., 2010. Thermal evaluation of vertical greenery systems for building walls. *Building and environment* 45 (3), 663–672.
- Yin, H., Kong, F., Middel, A., Dronova, I., Xu, H., James, P., 2017. Cooling effect of direct green façades during hot summer days: an observational study in Nanjing, China using TIR and 3DPC data. *Build. Environ.* 116, 195–206. <http://dx.doi.org/10.1016/j.buildenv.2017.02.020>.
- Zölch, T., Maderspacher, J., Wamsler, C., Pauleit, S., 2016. Using green infrastructure for urban climate-proofing: an evaluation of heat mitigation measures at the micro-scale. *Urban For. Urban Green.* 20, 305–316. <http://dx.doi.org/10.1016/j.ufug.2016.09.011>.